Available online at www.sciencedirect.com

ScienceDirect

IFAC PapersOnLine 58-19 (2024) 1078–1083

# Dynamic Process Force Simulation Model for Multi-Axis Milling Processes ⋆

**A. K. Rüppel [*] P. Ochudlo [**] M. Meurer [*] T. Bergs [*,***] S. Stemmler [**]**

[*] *Manufacturing Technology Institute (MTI), RWTH Aachen University, Aachen, Germany (e-mail: a.rueppel@mti.rwth-aachen.de, m.meurer@mti.rwth-aachen.de, t.bergs@mti.rwth-aachen.de).*

[**] *Institute of Automatic Control (IRT), RWTH Aachen University, Aachen, Germany (e-mail: p.ochudlo@irt.rwth-aachen.de, s.stemmler@irt.rwth-aachen.de)*

[***] *Fraunhofer Institute for Production Technology (IPT), Aachen, Germany (e-mail: thomas.bergs@ipt.fraunhofer.de)*

**Abstract:** Process forces are critical in cutting operations, affecting tool integrity and product quality. Milling is characterized by rapid process force fluctuations and unpredictable tool wear, hindering closed-loop control systems in industry, so far. Establishing control strategies require a high developmental effort. A simulation-based framework of the milling process eases the design of novel control strategies. However, this requires a realistic model of the entire system, which is currently lacking. In this work, a dynamic force simulation model for both three- and multi-axis milling is proposed. The results show relative errors of the model between 4.6 % and 10.6 %.



*Keywords:* Intelligent manufacturing systems, Modeling of manufacturing operations, Production planning and control, Flexible and reconfigurable manufacturing systems, force control

## 1. INTRODUCTION AND MOTIVATION

Milling is a highly flexible manufacturing process and often used to machine complex geometries. The high flexibility, however, results in vastly changing process conditions depending on tool geometry, programmed tool path, workpiece material, machine tool characteristics and more. Additionally, the probabilistic nature of tool wear results in an unpredictable process behavior. As a result, optimizing milling processes is still an ongoing research subject in both, science and industry.

One of the most important measured variables in milling processes is the process force. High process forces may result in tool damage or even tool breakage as well as low geometrical accuracy of the machined workpiece. If process forces are too low, however, the process is not operated at its technological optimum resulting in a less productive process (Liang et al. (2004)). In milling, process forces can abruptly change due to their dependency on the tool-workpiece-engagement, which is constantly varying during machining depending on the manufactured geometry as well as tool geometry and wear.

The unpredictability of the process forces during versatile machining operations make forces difficult to control in a closed-loop system using reactive controllers (Ulsoy and Koren (1993); Liang et al. (2004)). Recent approaches use model predictive control for force control in milling (Adams et al. (2016); Stemmler et al. (2016); Schwenzer et al. (2022)). All contributions named so far use the feed as the manipulated variable. All works are limited to three-axis milling processes, yet.

Introducing advanced control strategies to milling requires a model of the entire system, including aspects like machine tool dynamics, process forces, and transmission behavior of the measurement chain. The complexity of the model rises due to the more complex tool-workpiece engagement conditions in multi-axis milling processes. Additionally, employing table dynamometers for force measurement requires accounting for gravitational forces. However, very complex models result in significant simulation times rendering them impossible to be used in model-based controllers. A comprehensive simulation model for all effects on the one hand but simple enough for online usage on the other hand has not been published, yet.

Machine tool dynamics are typically modeled by considering a second order system with time delay, e.g. (Altintas (1994); Zuperl et al. (2012); Adams et al. (2016); Schwenzer et al. (2022)). To accurately model process forces, mechanistic force models are vastly used due to their good generalization and easy parametrization. Most works use proportional models (e.g. Berglind et al. (2017); Dongming et al. (2010); Layegh et al. (2012); Altintas (1994)); however the nonlinear model according to Kienzle may be generally more accurate (Adem et al. (2015); Kienzle (1952)). Measurement transmission characteristics as well as gravitational effects on the force measurement are not considered in most works. Only recently, advanced models

⋆ The presented research was funded by the Deutsche Forschungsgemeinschaft (DFG, German Research Foundation)—450794086.


10.1016/j.ifacol.2024.09.128

for some of these effects have been developed (Ochudlo et al. (2023); Rüppel et al. (2023)).

The proposed work introduces a comprehensive simulation model for multi-axis milling processes aimed at facilitating the design for closed-loop controllers. The method contributes to the overall objective of developing model predictive force control for multi-axis milling process. The work is to

- build a comprehensive model for all relevant effects: Machine tool dynamics, process force, tool runout, gravity, and transmission behavior of the measurement device,
- validate the model in both three- and multi-axis milling under different engagement conditions, and
- provide a simulation test bench for closed-loop control development.

The proposed model can be of interest in all fields, where dynamic and comprehensive milling process force models can be utilized, including: development of force controllers, machine tool and milling tool design, and process optimization. Simulation based rapid control prototyping significantly reduces the effort to develop control systems(Abel and Bollig (2013)).

The work is structured as follows: Section 2 describes the modeling approach including all relevant subsystems. In Section 3, the experimental setup for the simulation model is described as well as the machined geometries. Results of the validation as well as a discussion are detailed in Section 4. The work ends with a conclusion in Section 5.

## 2. MODELING APPROACH

Simulation-based development of closed-loop control systems requires comprehensive models of the system to be controlled. Cutting processes are complex systems with highly nonlinear transmission behavior. Modeling such processes requires the integration of multiple effects which can be described by different subsystems (c.f. Fig. 1). This work regards the following effects

- machine tool dynamics,
- mechanistic force model,
- tool runout,
- gravitational effects, and
- transmission behavior of measurement device.

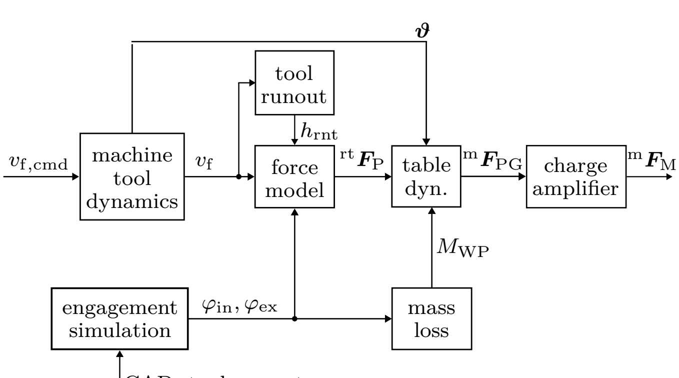


Fig. 1. Block diagram of the full system model

The commanded feed velocity $v_{\mathrm{f,cmd}}$ gets processed by the numerical control unit which actuates the physical machine tool axes. This results in a feed velocity $v_{\mathrm{f}}$ of the tool. The process force components ${}^{\mathrm{rt}}\boldsymbol{F}_{\mathrm{P}}$ [1] in rotating tool coordinate system are determined by the geometrical engagement conditions. The geometrical engagement is dependent on the position along the tool path. The engagement conditions get described by the angles $\varphi_{\mathrm{in}}$ and $\varphi_{\mathrm{ex}}$ of where the tool's teeth enter and exit the workpiece, respectively. Tool runout is explicitly considered, which alters the actual undeformed chip thickness by a runout specific chip thickness $h_{\mathrm{rnt}}$. The forces are measured using a table dynamometer, resulting in the necessity to correct gravitational effects dependent on the current mass $m_{\mathrm{WP}}$ of the workpiece and the angles $\boldsymbol{\vartheta}$ of the machine tool table around the A and C axis, respectively. Additionally, a rotation of the forces ${}^{\mathrm{m}}\boldsymbol{F}_{\mathrm{PG}}$ into the measurement coordinate system of the table dynamometer is further necessary. Finally, the BUTTERWORTH filter in the charge amplifier of the measurement chain is considered to determine the measured forces ${}^{\mathrm{m}}\boldsymbol{F}_{\mathrm{M}}$. The subsystems get further described in the following subsections.

### 2.1 Machine Model

In order to manipulate the machine tool's motion, manufacturers introduce different cascade control strategies to control position, velocity and motor currents. An introduction to control systems of machine tool drives is given e.g. by BRECHER and WECK (Brecher, 2022, pp. 129-135). With the aim of gathering an actuating system which is compatible with different machine tool's control systems, the existing cascade control is extended in this contribution. The desired feed rate obtained by position control is manipulated to actuate the machine tool while maintaining the existing motion control. Since the underlying control loops influence the axis dynamics, a physical model of the machine tool's motion is not practicable. Instead, a second-order lag system is used to approximate the axis dynamic, assuming a similar dynamic for each axis. The transfer function $G_{\mathrm{v}}$ reads

$$G_{\mathrm{v}} = \frac{V_{\mathrm{f}}(s)}{V_{\mathrm{f,cmd}}(s)} = \frac{K\omega_0^2}{s^2 + 2\zeta\omega_0 s + \omega_0^2}\mathrm{e}^{-sT_{\mathrm{d}}}, \quad (1)$$

with the static gain $K$, the damping ratio $\zeta$, the cutt-off frequency $\omega_0$ and the time delay $T_{\mathrm{d}}$. To find parameters describing the axis dynamic, a sequence of steps varying the step height and duration is generated for a combined x- and y-motion of the milling tool. It is worth noting that the desired velocity is reached after each step.

At first, the time delay is assessed based on the step responses as $T_{\mathrm{d}} = 0.06$ sec. The machine tool's control system is tuned to avoid overshoot of the feed velocity. Using the KIENZLE-model, overshoot of the machine tool's velocity leads to a force peak which is not observed in the experiments. Therefore, the identification is conducted limiting the damping ratio to $\zeta \geq 1$. The identified static gain reads $K = 1$. This is expected because the

[1] The superscript in front of the variable shows the coordinate system in which the variable is defined, rt: rotating tool coordinate system, mt: machine tool coordinate system, m: table dynamometer coordinate system.

machine tool's cascade control is designed to be offset-free. The damping ratio reads $\zeta = 1$, which is set as the lower bound in the identification. This indicates the optimal parameter to be $\zeta < 1$ approximating the axis motion by an underdamped system. Due to the absence of an overshoot in the measured velocity, the tendency of identifying an underdamped system is explained by the system's dynamic being non-linear. It is decided to use a non-ideal damping ratio for the approximation because unrealistic force peaks disturb the design of control strategies more severely than an inaccurate dynamic. The cut-off frequency of the machine model reads $\omega_0 = 64\,\frac{1}{\text{sec}}$. A validation of the machine model conducting random steps of both machine axes is depicted in Fig. 2, with the actual velocity $v_{\text{act}}$, the commanded velocity $v_{\text{cmd}}$ and the simulated velocity $v_{\text{sim}}$. The identified model fits the measurement well. The underlying cascade control has a higher dynamic for small changes (62.2 sec) compared to great changes (67.8 sec) of the commanded feed velocity. Therefore, the identified parameters are approximated for describing small and great steps adequately.

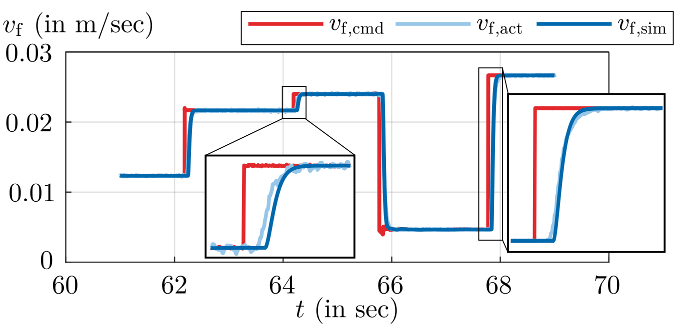


Fig. 2. Validation of the machine model conducting random steps of both machine axes simultaneously

*2.2 Mechanistic force model and runout*

To model the process force components in tangential and radial direction in the rotating tool coordinate system, the force model according to Kienzle is utilized

$$^{\text{rt}}F_{i,n,j} = k_i b_n {h_{n,j}}^{1-m_i}, \qquad \text{where } i \in \{t, r\}, \tag{2}$$

with the proportional model parameters $k_i$ and the exponential parameters $m_i$ (Kienzle (1952)). The model requires a numerical slicing of the tool (c.f. Fig. 3) in $N_{\text{s}}$ slices along the rotational axis for all $N_{\text{t}}$ teeth, so that every slice $n$ of every tooth $j$ has an own height $b_n$ and thickness $h_{n,j}$.

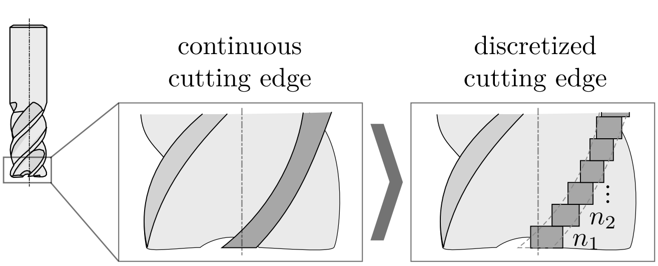


Fig. 3. Discretization of the cutting edges along the main rotational axis of the cutting tool

The cutting edge of every slice is assumed to be vertical. A slice which is not engaged has a height of zero, resulting in zero forces.

$$\begin{aligned} b_n &> 0, \quad \text{if slice } n \text{ is engaged} \\ b_n &= 0, \quad \text{if slice } n \text{ is not engaged} \end{aligned} \tag{3}$$

The forces are then transformed into machine tool coordinate system using the transformation

$$^{\text{mt}}\boldsymbol{F}_{\text{P},n,j} = {}^{\text{mt}}\mathbf{T}_{\text{rt}}(\varphi_{n,j}, \alpha)\,{}^{\text{rt}}\boldsymbol{F}_{\text{P},n,j}, \tag{4}$$

with the transformation matrix $^{\text{mt}}\boldsymbol{T}_{\text{rt}}$ depending on the feed direction angle $\alpha$ and the angle $\varphi_{n,j}$ of each slice of each tooth. The transformation matrix is given by

$$^{\text{mt}}\mathbf{T}_{\text{rt}} = \begin{pmatrix} \cos(\alpha - \varphi_{n,j}) & -\sin(\alpha - \varphi_{n,j}) \\ \sin(\alpha - \varphi_{n,j}) & \cos(\alpha - \varphi_{n,j}) \end{pmatrix}. \tag{5}$$

The actual undeformed chip thickness $h_{n,j}$ is dependent on the feed $f_{\text{t}}$ per tooth and the current angle $\varphi_{n,j}$ of the slice of the cutting edge as well as the effect of the runout $h_{\text{rnt},n,j}$. The equation reads

$$h_n = f_{\text{t}} \sin(\varphi_{n,j}) + h_{\text{rnt},n,j}. \tag{6}$$

To account for tool runout, the vastly used model according to Kline and DeVor is used to calculate the radial offset (Kline (1982)). The also proclaimed tilt of the tool gets neglected due to simplicity reasons resulting in the description of the runout by

$$\begin{aligned} h_{rnt,n,j} = 2\rho \sin\Bigg[\frac{2tan(\beta)}{D} b_n(n-0.5) - \lambda + \\ \ldots \frac{\pi}{N_t}(2j-3)\Bigg] \sin\left(\frac{\pi}{N_t}\right), \end{aligned} \tag{7}$$

with the direction angle $\lambda$, the distance $\rho$ from the center, and the number of teeth $N_t$. The determination, if a slice is engaged or not is based on the a-priori engagement simulation conducted using the software dPart from Fraunhofer Institute for Production Technology (IPT) (Ganser et al. (2021)).

The process force is the sum of the forces of all slices of all engaged teeth

$$^{\text{mt}}\boldsymbol{F}_{\text{P}} = \sum_{j=1}^{N_{\text{t}}} \sum_{n=1}^{N_{\text{s}}} {}^{\text{mt}}\boldsymbol{F}_{\text{P},n,j}. \tag{8}$$

*2.3 Influences of table rotation and dynamometer*

In a multi-axis milling operation using a table dynamometer, the process force get distorted by gravity and the transfer behavior of the measurement chain. The gravitational force $^{\text{mt}}\boldsymbol{F}_{\text{G}}$ is dependent on the current mass of the workpiece, which gets simulated a-priori according to the model by Rüppel et al. (2023). The current mass $M_{\text{WP},k}$ of the workpiece at position $k$ depends on the mass $M_{\text{WP},k-1}$

at previous position and removed mass $M_{\mathrm{r},k}$ from the last position

$$M_{\mathrm{WP},k} = M_{\mathrm{WP},k-1} - M_{\mathrm{r},k}(\varphi_{n,j}), \tag{9}$$

which depends on the current engagement condition and can be calculated from the engagement simulation. In order to rotate the process force in the measurement coordinate system and describe the gravitational influence on the measurement the rotation model according to Ochudlo et al. (2023) is used. Through the use of the measurement of the angular position of the machine tool table, the force components can be rotated into the coordinate system of the table dynamometer. The model is given by

$$^{\mathrm{m}}\boldsymbol{F}_{\mathrm{PG}} = \\ ...^{\mathrm{m}}\mathbf{T}_{\mathrm{mt}}(\vartheta_x, \vartheta_z)(^{\mathrm{mt}}\boldsymbol{F}_{\mathrm{P}} + {}^{\mathrm{mt}}\boldsymbol{F}_{\mathrm{G}}(M_{\mathrm{WP},k}, \vartheta_x, \vartheta_z)), \tag{10}$$

where $^{\mathrm{m}}\boldsymbol{T}_{\mathrm{mt}}$ is the transformation matrix depending on the current table orientation $\vartheta_x$ around the A-axis and $\vartheta_z$ around the C-axis

$$^{\mathrm{m}}\mathbf{T}_{\mathrm{mt}} = \mathbf{T}_{\mathrm{z}}(\vartheta_{\mathrm{z}})\mathbf{T}_{\mathrm{x}}(\vartheta_{\mathrm{x}}), \tag{11}$$

with

$$\mathbf{T}_{\mathrm{x}}(\vartheta_{\mathrm{x}}) = \begin{pmatrix} 1 & 0 & 0 \\ 0 & \cos(\vartheta_{\mathrm{x}}) & -\sin(\vartheta_{\mathrm{x}}) \\ 0 & \sin(\vartheta_{\mathrm{x}}) & \cos(\vartheta_{\mathrm{x}}) \end{pmatrix}, \tag{12}$$

and

$$\mathbf{T}_{\mathrm{z}}(\vartheta_{\mathrm{z}}) = \begin{pmatrix} \cos(\vartheta_{\mathrm{z}}) & -\sin(\vartheta_{\mathrm{z}}) & 0 \\ \sin(\vartheta_{\mathrm{z}}) & \cos(\vartheta_{\mathrm{z}}) & 0 \\ 0 & 0 & 1 \end{pmatrix}. \tag{13}$$

Finally, the charge amplifier includes a fourth order BUTTERWORTH filter with a cut-off frequency $f_{\mathrm{c}} = 300\,\mathrm{Hz}$ which is necessary to avoid aliasing effects in the measurement of the process forces. The filter is modeled explicitly by using the digital transfer function

$$G_{\mathrm{BW}}(z) = \frac{b_0 + b_1 z^{-1} + b_2 z^{-2} + b_3 z^{-3} + b_4 z^{-4}}{a_0 + a_1 z^{-1} + a_2 z^{-2} + a_3 z^{-3} + a_4 z^{-4}}, \tag{14}$$

with the sample rate $T_s = 5\,\mathrm{kHz}$, as the implementation of the force model needs to be in discrete form and, therefore, only discrete forces are simulated. The parameters were chosen using the Matlab Signal Processing Toolbox and are given in Table 1.

Table 1. Parameters of the low pass filter

| $a_0$ | $a_1$ | $a_2$ | $a_3$ | $a_4$ | $b_0$ | $b_1$ | $b_2$ | $b_3$ | $b_4$ |
|---|---|---|---|---|---|---|---|---|---|
| 1 | -3 | 3.5 | -1.9 | 0.4 | 8e-4 | 3e-3 | 5e-3 | 3e-3 | 8e-4 |

Using the transfer function, the process force get transferred to the measured force according to

$$^{\mathrm{m}}\boldsymbol{F}_{\mathrm{M}} = G_{\mathrm{BW}}(z)\mathbf{I}^{\mathrm{m}}\boldsymbol{F}_{\mathrm{PG}}, \tag{15}$$

in x- and y-direction of the table dynamometer. $\mathbf{I}$ is the identity matrix.

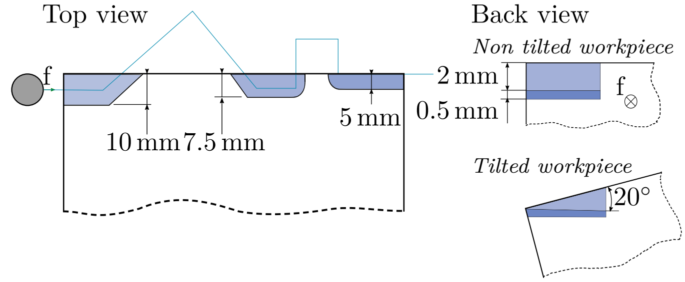


Fig. 4. Machined test geometries in both three-axis (non tilted) and multi-axis (tilted) milling scenarios

## 3. EXPERIMENTAL SETUP AND MODEL CALIBRATION

Experiments have been conducted on a Mazak VARIAXIS i-600 machine tool with a two fluted cemented carbide end mill at a helical angle of $\beta = 35°$. To account for different engagement conditions in both three-axis and multi-axis milling, the test geometry shown in Fig. 4 was machined while the table was horizontal for three-axis experiments and under an angle of $\vartheta_{\mathrm{x}} = 20°$ for multi-axis experiments.

The forces were measured using a Kistler 9255B table dynamometer at a rate of 5 kHz with a Kistler charge amplifier Type 5070. The force and runout model is highly dependent on the model parameters $k_i, m_i, \rho$, and $\lambda$. The parameters were identified using least squares algorithm on data acquired in a test cut, which was excluded from further model validation. The cutting edge was numerically sliced with a slice height of $b_n = 0.1\,\mathrm{mm}$, which has been chosen according to SCHWENZER (Schwenzer (2022)). The identified parameters are shown in Table 2. The identification was based on one revolution of all areas with constant engagement conditions along the tool path.

Table 2. Identified force and runout model parameters

| $k_{\mathrm{t}}$ (in N/mm²) | $k_{\mathrm{r}}$ (in N/mm²) | $m_{\mathrm{t}}$ (-) | $m_{\mathrm{r}}$ (-) | $\rho$ (in °) | $\lambda$ (in µm) |
|---|---|---|---|---|---|
| 1203 | 281 | 0.26 | 0.39 | 92 | 27.2 |

The initial mass was measured by $M_{\mathrm{WP},1} = 6.151\,\mathrm{kg}$ and was mathematically adjusted after every cut. All experiments were conducted at a constant cutting velocity of $v_{\mathrm{c}} = 80\,\mathrm{m\,min^{-1}}$.

## 4. VALIDATION AND RESULTS

To validate the model, a total of four experiments have been conducted with two different feed velocities of $v_{\mathrm{f},1} = 266\,\mathrm{mm\,min^{-1}}$ and $v_{\mathrm{f},2} = 330\,\mathrm{mm\,min^{-1}}$ both at three- and multi-axis milling conditions. Fig. 5 shows results for a three-axis cut at $v_{\mathrm{f},1}$ in both x- and y-direction in measurement coordinate system. The estimation of the variable $\boldsymbol{F}$ is denoted as $\check{\boldsymbol{F}}$.

The model shows good agreement to the measured forces in both directions and varying engagement conditions. The explicit consideration of the BUTTERWORTH filter improves the model significantly in changing tool-workpiece engagement conditions or when the tool is not in full

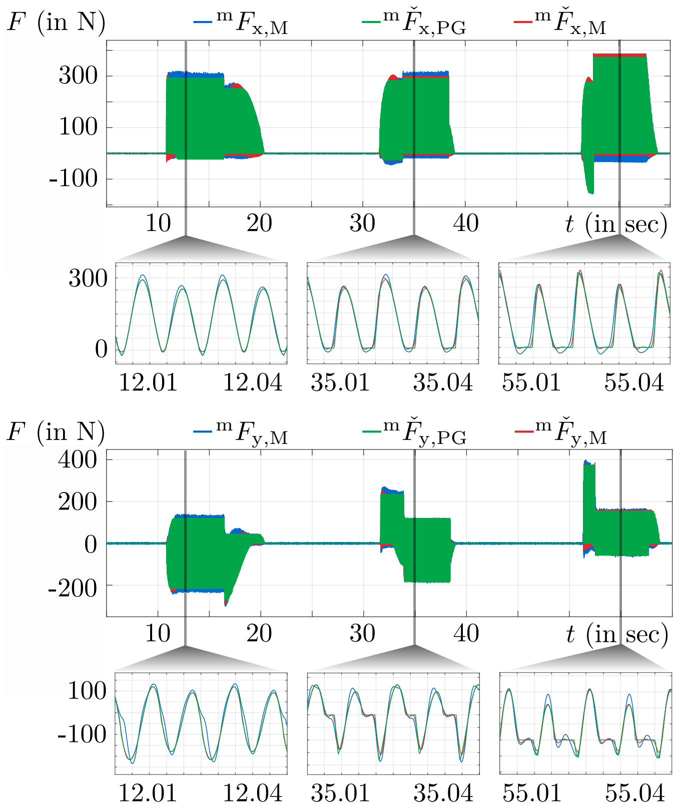


Fig. 5. Validation of measured forces in three-axis milling at $v_{\mathrm{f},1} = 266$ mm min$^{-1}$ using experimental data

immersion. The filter leads to an overshoot of the forces compared to the non filtered case, which shows significant force alterations when the force changing rate is high. This especially shows when no tooth is engaged or at peek force of each cut, framing it very important for modeling maximum forces per revolution. The effect is small when the tool is in full immersion. The model shows good agreement in both dynamics and maximum forces per revolution. However, small deviations in the third engagement are visible due to different runout. Additionally, different deviations in different engagement conditions hint to engagement specific coefficients of the force and runout model.

For multi-axis milling at $v_{\mathrm{f},2}$, results are shown in Fig. 6. Here, the model shows good quality concerning dynamics in all engagement conditions as well. However, the accuracy of maximum force per revolution is worse than in three-axis milling. Explanations for this may be inaccuracies caused by the rotation model as well as the numerical slicing of the tool which results in higher inaccuracies due to the variable engagement along the tool rotation axis. Table 3 shows the metrics for the model evaluation. Air cuts were excluded from the results.

In all experiments, the mean absolute error $\Delta\overline{F}$ is between 11 N and 21 N. For the desired purpose of designing a control system, the maximum force per revolution $F_{\mathrm{max,rev}}$ is a more relevant metric. The absolute model error $\Delta F_{\mathrm{max,rev}}$ is between 16 N and 31.7 N, resulting in relative errors $\Delta F_{\mathrm{max,rev}}/F_{\mathrm{max}}$ between 4.7 % and 10.6 %. In general, the model shows better accuracy with a modeled Butterworth filter. Deviations are also higher in multi-axis milling caused by the bigger influence of the numerical slicing of the tool when the engagement is variable along the tool axis as well as the analytical force rotation model.

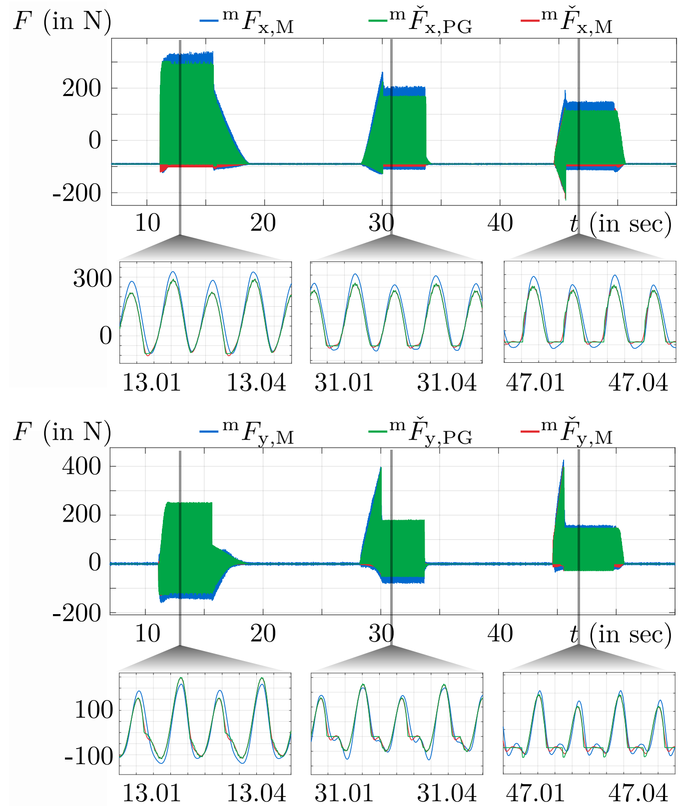


Fig. 6. Validation of process forces in multi-axis milling at $v_{\mathrm{f},2} = 330$ mm min$^{-1}$ using experimental data

Table 3. Results of the model accuracy in different cutting scenarios and at different feed velocities.

| Dataset | LP filter | force comp. | $\Delta\overline{F}$ [N] | $\Delta F_{\mathrm{max,rev}}$ [N] | $\frac{\Delta F_{\mathrm{max,rev}}}{F_{\mathrm{max}}}$ [%] |
|---|---|---|---|---|---|
| three-ax. at $v_{\mathrm{f},1}$ | No | $F_{\mathrm{x}}$ | 13.4 | 17.4 | 4.7 |
| | | $F_{\mathrm{y}}$ | 16.5 | 16.0 | 4.3 |
| three-ax. at $v_{\mathrm{f},1}$ | Yes | $F_{\mathrm{x}}$ | 12.7 | 14.7 | 3.8 |
| | | $F_{\mathrm{y}}$ | 15.2 | 15.0 | 3.9 |
| three-ax. at $v_{\mathrm{f},2}$ | Yes | $F_{\mathrm{x}}$ | 15.5 | 21.9 | 4.9 |
| | | $F_{\mathrm{y}}$ | 11.5 | 13.8 | 3.1 |
| multi-ax. at $v_{\mathrm{f},1}$ | Yes | $F_{\mathrm{x}}$ | 15.2 | 20.9 | 8.4 |
| | | $F_{\mathrm{y}}$ | 12.6 | 15.9 | 4.6 |
| multi-ax. at $v_{\mathrm{f},2}$ | Yes | $F_{\mathrm{x}}$ | 21.0 | 31.7 | 10.6 |
| | | $F_{\mathrm{y}}$ | 15.3 | 17.0 | 4.3 |

Overall, the model proves to simulate dynamic cutting process forces with high accuracies. The deviations are partly due to numerical inaccuracies, resulting in the slicing of the cutting edge along the tool path. Increase of the number of slices, however, results in higher computation time, which makes the model less appropriate for simulation-based development.

Furthermore, all experiments revealed rather engagement specific parameters of the mechanistic force and runout model. Additional experiments will be conducted where force and runout model parameters get identified online as has been done by SCHWENZER et al. using an ensemble KALMAN filter (Schwenzer et al. (2022)).

## 5. CONCLUSION AND OUTLOOK

This work provides a simulation model for dynamic process forces for arbitrary tool paths in end milling processes to be used, among others, for design of closed-loop force control systems. A model consists of different subsystems, including machine tool dynamics, mechanistic force and runout models as well as mass loss, force rotation and low pass filter model. The model shows good agreement in both three- and multi-axis cutting experiments under different feed velocities with relative errors between 3.1 % and 10.6 %. Further improvement can be done by identifying model parameters online or by enhancing model resolution.

Next steps can be the integration of the rotational axes into the model of the machine tool to enable simulation of milling processes, where all five axes are simultaneously operated. This might require a different model for the rotational axes. Furthermore the current model is restricted to tools with constant diameter. While simulation of cutting tools with varying diameter (like ball or conical end mills) is possible, it has not been validated, yet, and might require an adjustment of the force model to account for changing cutting velocity along the tool axis.

## REFERENCES


Abel, D. and Bollig, A. (2013). *Rapid control prototyping: Methoden und Anwendungen ; mit 16 Tabellen*. Springer, Berlin and Heidelberg.

Adams, O., Klocke, F., Schwenzer, M., Stemmler, S., and Abel, D. (2016). Model-based Predictive Force Control in Milling – System Identification. *Procedia Technology*, 26, 214–220. doi:10.1016/j.protcy.2016.08.029.

Adem, K.A.M., Fales, R., and El-Gizawy, A.S. (2015). Identification of cutting force coefficients for the linear and nonlinear force models in end milling process using average forces and optimization technique methods. *The International Journal of Advanced Manufacturing Technology*, 79(9-12), 1671–1687. doi:10.1007/s00170-015-6935-3.

Altintas, Y. (1994). Direct adaptive control of end milling process. *International Journal of Machine Tools and Manufacture*, 34(4), 461–472. doi:10.1016/0890-6955(94)90078-7.

Berglind, L., Plakhotnik, D., and Ozturk, E. (2017). Discrete Cutting Force Model for 5-Axis Milling with Arbitrary Engagement and Feed Direction. *Procedia CIRP*, 58, 445–450. doi:10.1016/j.procir.2017.03.250.

Brecher, C. (2022). *Machine Tools Production Systems 3: Mechatronic Systems, Control and Automation*. Lecture Notes in Production Engineering Ser. Springer Fachmedien Wiesbaden GmbH, Wiesbaden. URL `https://ebookcentral.proquest.com/lib/kxp/detail.action?docID=6826384`.

Dongming, G., Fei, R., and Yuwen, S. (2010). An Approach to Modeling Cutting Forces in Five-Axis Ball-End Milling of Curved Geometries Based on Tool Motion Analysis. *Journal of Manufacturing Science and Engineering*, 132(4). doi:10.1115/1.4001420.

Ganser, P., Venek, T., Rudel, V., and Bergs, T. (2021). DPART – A Digital Twin Framework for the Machining Domain. *MM Science Journal*, 2021(5), 5134–5141. doi:10.17973/MMSJ.2021_11_2021168.

Kienzle, O. (1952). Die Bestimmung von Kräften und Leistungen an spanenden Werkzeugmaschinen. VDI-Z, 299–305. VDI-Verlag.

Kline, W.A. (1982). *The prediction of cutting forces and surface accuracy for the end milling process*. PhD Thesis, University of Illinois at Urbana-Champaign, Illinois.

Layegh, K.S.E., Erdim, H., and Lazoglu, I. (2012). Offline Force Control and Feedrate Scheduling for Complex Free Form Surfaces in 5-Axis Milling. *Procedia CIRP*, 1, 96–101. doi:10.1016/j.procir.2012.04.015.

Liang, S.Y., Hecker, R.L., and Landers, R.G. (2004). Machining Process Monitoring and Control: The State-of-the-Art. *Journal of Manufacturing Science and Engineering*, 126(2), 297–310. doi:10.1115/1.1707035. URL `https://asmedigitalcollection.asme.org/manufacturingscience/article/126/2/297/446052/Machining-Process-Monitoring-and-Control-The`.

Ochudlo, P., Rüppel, A.K., Stemmler, S., Bergs, T., and Abel, D. (2023). Model-Based Determination Of Process Force In Multi-Axis Milling. In *Proceedings of the 9th World Congress on Mechanical, Chemical, and Material Engineering*, World Congress on Mechanical, Chemical, and Material Engineering. Avestia Publishing. doi:10.11159/mmme23.117.

Rüppel, A.K., Ochudlo, P., Bickel, M., Stemmler, S., Bergs, T., and Abel, D. (2023). Mass Loss and Displacement Modeling for Multi-Axis Milling. *Procedia CIRP*. URL `https://arxiv.org/abs/2311.06847`.

Schwenzer, M. (2022). *Closing the Loop of Model Predictive Force Control in Milling with Ensemble Kalman Filtering*. Dissertation, RWTH Aachen, Aachen.

Schwenzer, M., Stemmler, S., Ay, M., Rüppel, A.K., Bergs, T., and Abel, D. (2022). Model predictive force control in milling based on an ensemble Kalman filter. *Journal of Intelligent Manufacturing*, 33(7), 1907–1919. doi:10.1007/s10845-022-01931-2.

Stemmler, S., Abel, D., Adams, O., and Klocke, F. (2016). Model Predictive Feed Rate Control for a Milling Machine. *IFAC-PapersOnLine*, 49(12), 11–16. doi:10.1016/j.ifacol.2016.07.542.

Ulsoy, A.G. and Koren, Y. (1993). Control of Machining Processes. *Journal of Dynamic Systems, Measurement, and Control*, 115(2B), 301–308. doi:10.1115/1.2899070. URL `https://asmedigitalcollection.asme.org/dynamicsystems/article/115/2B/301/417440/Control-of-Machining-Processes`.

Zuperl, U., Cus, F., and Reibenschuh, M. (2012). Modeling and adaptive force control of milling by using artificial techniques. *Journal of Intelligent Manufacturing*, 23(5), 1805–1815. doi:10.1007/s10845-010-0487-z.